

Manipulation of the Elastic Modulus of Polymers at the Nanoscale: Influence of UV–Ozone Cross-Linking and Plasticizer

Jessica M. Torres,[†] Christopher M. Stafford,[‡] and Bryan D. Vogt^{†,*}

[†]Department of Chemical Engineering, Arizona State University, Tempe, Arizona 85284 and [‡]Polymers Division, National Institute of Standards and Technology, Gaithersburg, Maryland 20899

Nature utilizes hierarchical structuring from the atomic to macroscopic scales to create highly robust, functional materials such as gecko feet for adhesion^{1,2} and lotus leaves for self-cleaning.^{3–5} These cues from nature are being exploited in biomimetic designs, such as in polymeric structures fabricated using imprint lithography to create nonfouling surfaces based upon sharkskin motifs.⁶ One critical parameter for the efficacy of these designs is the mechanical properties of the components comprising the hierarchical structures, especially those at the nanoscale.^{7–9} Additionally, mechanical robustness of polymers under nanoscale confinement is critical for numerous developed and emerging applications including photonics,¹⁰ microelectronics,¹¹ nonlinear optics,¹² self-cleaning surfaces,^{3–5} and biosensors.¹³ Thin films provide a simple geometry to examine polymers confined to nanometer length scales. However, studies of polymer thin films have primarily focused on elucidating the effect of confinement on the glass transition temperature (T_g),^{14–18} while their mechanical properties have been investigated with conflicting results as to the impact of confinement on elastic modulus of soft materials: the modulus has been reported to increase,¹⁹ decrease,^{20–23} or not change,^{24–26} similar to results from initial polymer thin film T_g measurements.²⁷ In the case of thin film T_g , some of the initial conflicting results can now be rationalized by differences in the polymer–substrate interaction.²⁸ Similarly, the nature of the probe interaction for indentation measurements has been shown to impact the observed mechanical proper-

ABSTRACT The mechanical stability of polymeric nanostructures is critical to the processing, assembly, and performance of numerous existing and emerging technologies. A key predictor of mechanical stability is the elastic modulus. However, a significant reduction in modulus has been reported for thin films and nanostructures when the thickness or size of the polymer material decreases below a critical length scale. Routes to mitigate or even eliminate this reduction in modulus, and thus enhancing the mechanical stability of polymeric nanostructures, would be extremely valuable. Here, two routes to modulate the mechanical properties of polymers at the nanoscale are described. Exposure to ultraviolet light and ozone (UVO) cross-links the near surface region of high molecular mass PS films, rendering the elastic modulus independent of thickness. However, UVO cannot eliminate the decrease in modulus of low molecular mass PS or PMMA due to limited reaction depth and photodegradation, respectively. Alternatively, the thickness dependence of the elastic modulus of both PS and PMMA can be eliminated by addition of dioctyl phthalate (DOP) at 5% by mass. Furthermore, an increase in modulus is observed for films with thicknesses less than 30 nm with 5% DOP by mass in comparison to neat PS. Although DOP acts as a plasticizer for both PS and PMMA in the bulk, evidence indicates that DOP acts as an antiplasticizer at the nanoscale. By maintaining or even increasing the elastic modulus of polymers at the nanoscale, these methods could lead to improved stability of polymeric nanostructures and devices.

KEYWORDS: thin films · elastic modulus · wrinkling · polymers · confinement · surface modification

ties.¹⁹ Recently, two different noncontact approaches, based upon wrinkling of thin films and capillary deformation of nanostructures, have shown a decrease in the elastic modulus of PMMA when confined to the nanometer scale.^{20,21,29} Interestingly, a decrease in the modulus has been predicted by molecular dynamic simulations, and the thickness at which deviations from the bulk value occur is found to scale directly with the quench depth into the bulk glass.³⁰ This prediction agrees well with the measured thin film moduli for a family of polymethacrylates with different bulk T_g values.³¹ This decreased modulus is believed to be caused by coupling of the cooperative dynamics at the free surface into the film.^{32,33}

*Address correspondence to bryan.vogt@asu.edu.

Received for review April 8, 2010 and accepted August 05, 2010.

Published online August 16, 2010. 10.1021/nn100720z

© 2010 American Chemical Society

Many physical properties of polymers are observed to deviate from the bulk values near interfaces, including viscosity,³⁴ elastic modulus,²² compliance,¹⁹ and chain relaxation^{35,36} (including surface T_g).¹⁴ In studies of polymer thin films, PS has been generally examined as a model system. A significant decrease in the modulus of PS has been reported within 5–10 nm of the free surface.^{22,23} Additionally, several reports have demonstrated that the surface dynamics are much faster than the bulk for PS films, consistent with a reduced surface modulus.^{37,38} Ellison and Torkelson utilized pyrene-labeled layers within PS films to examine the distribution of T_g values, with a gradient in T_g extending approximately 40 nm below the free surface.¹⁴ These results indicate that the free surface of a polymer has properties that differ from the bulk, which could lead to a decrease in the mechanical integrity of polymeric nanostructures having high surface to volume ratios. Indeed, Torkelson and co-workers demonstrated that the T_g of lithographically patterned PMMA films is less than that observed for unpatterned films of identical thickness.³⁹ Thus, minimizing this free surface effect is necessary for generating robust polymeric nanostructures. One route to decrease the influence of the soft surface is to increase the bulk T_g of the polymeric system.^{30,31} However, high T_g polymers can be difficult to process due to difficulties with annealing and removal of processing history; for example, nanoimprint lithography requires processing at high temperatures to reduce the viscosity of the polymer melt and to enable flow of the polymer into the nanostructured mold, but this processing temperature must be below the degradation temperature of the polymer.

Alternatively, the surface of the confined films and/or nanostructures could be chemically modified in a manner that improves its mechanical integrity. One common route to the modification of polymer surfaces is through use of ultraviolet (UV) radiation. Koberstein and co-workers used UV radiation coupled with molecular oxygen (UVO) to create inorganic oxide coatings on surfaces, which should be significantly more mechanically robust than the precursors.⁴⁰ UVO treatment simultaneously utilizes UV light and ozone produced *in situ* to photochemically modify the surface. In cases where oxidation and cross-linking occur, such as for poly(dimethylsiloxane) (PDMS) and PS, UVO is known to improve adhesion, wettability, and toughness of polymers through modification of the near surface region, ≈ 5 nm.^{41,42} However, other polymers, such as PMMA, predominantly undergo chain scission rather than cross-linking; thus UVO treatment would not be appropriate for all polymers.⁴²

Recently, de Pablo and co-workers used simulations to identify an alternative route to eliminate the observed decrease in modulus of thin films and nanostructures: the use of an antiplasticizer.⁴³ These simulations suggest that, upon the confinement of a polymer/dilu-

ent system, both the initial energy barriers for chain relaxation and T_g are unchanged, unlike the neat polymer when confined to a thin film.⁴⁴ Simulations studying particle movement within confined polymer films suggest the addition of an antiplasticizer eliminates the propagation of free surface effects by making the film and near surface homogeneous, thus decreasing the near surface length scale for cooperative motion required for polymer relaxation.^{14,43} Recently, antiplasticization of lithographically patterned polymer nanostructures has been demonstrated.⁴⁵ Deformation and collapse of these features from capillary forces indicated that the modulus of PMMA is decreased when the beam width is less than 50 nm, but addition of 5% antiplasticizer can increase the modulus by 20% irrespective of the feature size.⁴⁵ However, plasticizers, rather than antiplasticizers, are commonly utilized in nanoimprint lithography.⁴⁶ Ellison *et al.* illustrated that a plasticizer, dioctyl phthalate (DOP), can effectively eliminate any finite size effects on T_g of PS.⁴⁷ It is presently unclear if a small molecule that acts as a plasticizer in the bulk can actually lead to antiplasticization and enhancement of mechanical properties in polymer thin films and nanostructures.

In this article, we examine the efficacy of two different processing routes, UVO treatment and addition of a bulk plasticizer, to increase the moduli of ultrathin (<30 nm) PS and PMMA films. Elastic moduli are elucidated using the wrinkling instability of a thin polymer film on an elastic substrate.^{20,48} The modulus of polymer films as thin as 5 nm has been determined with this metrology.^{20,21} To understand molecular mass effects, both a high molecular mass PS and an oligomer of PS are studied using both processing routes (UVO treatment and addition of plasticizer). We demonstrate that low concentrations of a plasticizer can effectively eliminate the observed thickness dependence of the elastic modulus in thin polymer films without significantly decreasing the modulus. A more complex situation arises with UVO treatment, where the efficacy of this method is dependent upon chemistry (PS vs PMMA) and molecular mass (high vs low). These experimental results can be explained in terms of near surface effects and the impact of the processing routes explored here on polymer properties in the vicinity of a free interface.

RESULTS AND DISCUSSION

Several reports on the impact of confinement on the elastic modulus of polymer thin films and nanostructures suggested a decreased modulus when measured using noncontact methodologies.^{20,21,29,31} This reduction in modulus is consistent with a purported liquid-like free surface layer that is dependent on both the structure and properties of the bulk polymer.^{14,49} Consistent with these prior measurements,^{21,31} we observe a decrease in elastic modulus for PS when the film thickness (h_f) is decreased below a critical threshold value, as shown in Figure 1. One interesting feature is that the critical thickness at which deviations in the

elastic modulus are observed is dependent upon molecular mass of the PS.³¹ Using a bilayer approach^{20,49} to model a polymer film as having a soft surface layer of finite thickness, δ , with the remainder of the polymer film behaving similar to the bulk, we find that the apparent thickness of the soft surface layer increases from $\delta \approx 5$ nm to $\delta \approx 25$ nm when the number-average relative molecular mass (M_n) of PS is decreased from 492 kg/mol (Figure 1b) to 1.3 kg/mol (Figure 1a). It is important to note that the large size of δ for the low molecular mass PS is significantly larger than typically reported for surface layers in polymer thin films, but Priestley *et al.* showed even larger length scales for the impact of the surface on physical aging.⁵⁰ Similar to the change in δ , the length scale below which deviations from the bulk-like modulus occur shifts from approximately 50 nm for the high M_n PS to greater than 60 nm for the low M_n PS, which suggests that the observed decrease in modulus is a result of a thin mechanically weak surface layer. It should be noted that McKenna and co-workers using bubble inflation of polystyrene films found an increase in the compliance in the rubbery regime for ultrathin films, while no thickness dependence in the glassy modulus is observed.²⁶ It is difficult to assess why there is such a disparity in the mechanical behavior of thin PS films between these noncontact techniques, but it could be related to the time scales of the measurement; the bubble inflation probes relatively long time scales in comparison to the high-frequency modulus determined from wrinkling. Similarly, there is significant difference in the measurement time scales for DSC and ellipsometry measurements, with generally no change in T_g reported from DSC,⁵¹ while a decrease in T_g is determined from ellipsometric measurements⁵² of ultrathin PS films.

If the surface of the polymer is indeed the source of the decreased modulus, one potential route to overcome the decreased mechanical robustness is to cross-link the surface of the PS in order to decrease polymer mobility and increase the surface stiffness. One well-established route to cross-link PS surfaces is through exposure to UVO.⁵³ The impact of exposure to UVO (broad-band UV from a low-pressure mercury lamp) on the thickness dependence of the modulus for 1.3 and 492 kg/mol PS films is shown in Figure 1. UVO treatment for the conditions examined does not significantly impact the film thickness. Interestingly, for 1.3 kg/mol PS films (Figure 1a), the observed modulus decrease in the unexposed nanoconfined PS film is preserved even after UVO exposure: at $h_f > 50$ nm, the modulus is thickness-independent, while the modulus begins to decrease significantly as the film thickness is decreased below 50 nm. Thus, the UVO treatment is unable to eliminate the effects of nanoconfinement on the elastic modulus of low molecular mass PS films. However, compared to the unexposed low molecular mass PS, the thicker (>50 nm) UVO-exposed films show an overall increase in apparent elastic modulus from $E_f(t_{\text{UVO}} = 0 \text{ s}) \approx 1.06$ GPa to $E_f(t_{\text{UVO}} > 0 \text{ s}) \approx 1.87$ GPa, as-

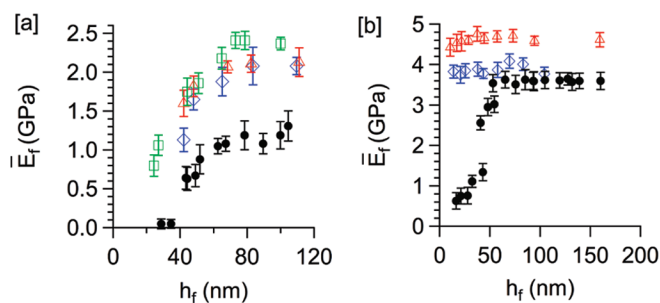


Figure 1. (a) Modulus as a function of film thickness for 1.3 kg/mol PS: pristine (●), after 30 s UVO exposure (◇), after 60 s UVO exposure (△), and after 90 s UVO exposure (□). (b) Modulus as a function of film thickness for 493 kg/mol PS: pristine (●), after 30 s UVO exposure (◇), and 60 s UVO exposure (△). The error bars represent one standard deviation of the data, which is taken as the experimental uncertainty of the measurement.

suming a Poisson's ratio, ν_f , of 0.33. Note that Figure 1 reports the strain-plane modulus, $\bar{E}_f = E_f/(1 - \nu_f^2)$. Similarly, the 492 kg/mol PS films exhibit an increase in overall modulus when exposed to UVO, but the modulus becomes independence of thickness after UVO exposure of 30 and 60 s. The bulk elastic modulus of unexposed PS is approximately 3.2 GPa, which increases to approximately 3.5 and 4.0 GPa after 30 and 60 s of UVO exposure, respectively. Additionally, a bulk-like modulus is measured for films as thin as 15 nm after UVO exposure; this is counter to neat polymers that we have examined where a decrease in modulus relative to the bulk is observed at this length scale.^{20,29,31} To explain the molecular mass dependency on the efficacy of UVO treatment, an understanding of the effects of UVO on the properties of PS surfaces is required.

Fortuitously, the UVO surface treatment of polymers has been widely studied and the mechanism of surface modification has been established.^{40–42,53} Ozone (or atomic oxygen) initially breaks molecular bonds on the surface of the polymer, allowing for the addition of oxygen atoms.⁵⁴ For short exposure times ($t_{\text{UVO}} < 60$ s), the atomic concentration of oxygen increases linearly with time to approximately 6% after 60 s exposure.⁴¹ This work uses an identical UVO model to the prior detailed study on the oxidation of PS surfaces,⁴¹ but the sample to source distance is much less (≈ 1 cm here compared to 4 cm). With the exposures used, it is expected that a maximum of 7 atom % oxygen will be incorporated into the films.⁴¹ Atomic oxygen reacts with the polymer chain by an insertion reaction to form carbonyl groups or through the removal of hydrogen from the chain to yield a carbon radical; this carbon radical can lead to the formation of carboxyl groups and enables cross-linking between polymer chains.^{41,42} As oxygen is required for these reactions, the diffusion of oxygen through the film is required; cross-linking of the surface limits the diffusion of oxygen and leads to an apparent limitation of the modification to the near surface region extending approximately 5 nm into the film.⁴¹ In addition to the cross-linking induced by oxygen, UV light can also cross-link

the PS matrix;^{55–57} however, the penetration depth for effective cross-linking of PS is 1–2 μm .⁵⁵ Thus, for the thin films examined here, UV light can penetrate through the film and cross-link the bulk of the PS. However, the rate of cross-linking of PS from UV light alone is quite slow⁵⁵ in comparison to ozone, so the bulk will only be lightly cross-linked even after 90 s of exposure. With these prior results in mind, it is possible to interpret the thin film moduli data for the PS films exposed to UVO as shown in Figure 1. For high molecular mass PS (492 kg/mol), the free surface layer ($h_f \approx 5$ nm) having a reduced modulus should be completely oxidized and cross-linked by ozone based on the observed diffusion-limited penetration depth of ≈ 5 nm for molecular oxygen during UVO exposure. Conversely, the UVO treatment of low molecular mass PS (1.3 kg/mol) does not eliminate the thickness-dependent modulus. However, the lower molecular mass PS has a significantly larger surface layer ($\delta \approx 25$ nm) that cannot be oxidized through its entire thickness by ozone, but the UV-induced cross-linking can occur through the whole film thickness. The thin film modulus behavior can be qualitatively understood by examining the depth-dependent cross-link density in PDMS using UV with and without ozone.⁵⁸ In this case, significant surface oxidation is only observed within the first 5 nm, which is attributed to ozone. However, a weaker cross-linking response due to UV alone penetrates approximately 100 nm into the film.⁵⁸ The large density change for PDMS enables this depth dependence to be elucidated. There are significant structural differences between PDMS and PS with PS being a much stronger absorber in the UV due to its aromaticity, but UV only to cross-link thin films (< 100 nm) of PS-*b*-PMMA utilizes a dose of 25 J/cm² (would correspond to 15 min exposure here),⁵⁹ which is consistent with the much slower cross-linking by UV alone. Thus, the weaker cross-linking through the film thickness based on UV exposure is likely responsible for a major of the increase in modulus observed for the thick films. However, as the near surface has enhanced mobility³⁷ and is mechanically more compliant, oxidation is likely necessary to mechanically enhance this region of the film to the same extent as the bulk. If the near surface became significantly stiffer than the bulk of the film during UVO exposure, the moduli would then increase as film thickness is decreased, which is not observed. For this reason, the modulus of near surface of the UVO-modified PS must be similar to that of the bulk for the high molecular mass PS that has been UV cross-linked. In contrast, the modulus for the thinner films of the low molecular mass PS decreases for the thinner films. This thickness-dependent behavior indicates that a portion of these films exhibits a lower modulus. As the modulus is constant for films thicker than approximately 60 nm for a given UVO exposure, lack of UV penetration through the film cannot account for this difference. However, the difference in the size scale of the softer near surface region in the neat PS films appears to match the observed dependence on

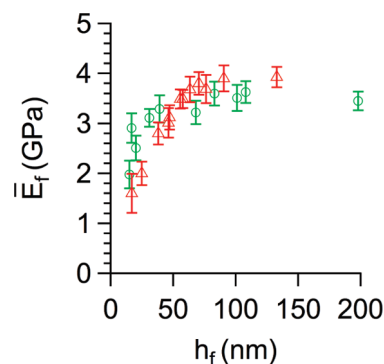


Figure 2. Modulus as a function of film thickness for 91 kg/mol PMMA: pristine (Δ) and after 30 s UVO exposure (\circ). The error bars represent one standard deviation of the data, which is taken as the experimental uncertainty of the measurement.

molecular mass of PS for the thin film elastic modulus dependent upon the finite penetration depth of the ozone during UVO treatment.

To further investigate the influence of UVO treatment on the mechanical properties of confined polymers, thin films of PMMA were also examined. The impact of UVO exposure on the elastic modulus of PMMA is shown in Figure 2; the UVO-treated PMMA remains statistically invariant to the unexposed PMMA at identical thickness. During exposure to UV radiation, cross-linking and chain scission occur simultaneously, but the dominance of either process is a function of the polymer structure.^{42,60,61} Unlike the predominance of cross-linking processes for PS, PMMA primarily undergoes chain scission of the methyl esters followed by the generation of one unsaturated bond in the polymer chain under UV irradiation.⁶¹ This difference in behavior has been exploited in block copolymer lithography using PS and PMMA segments to create a nanoporous template upon removal of the PMMA fragments.⁵⁹ Since the surface of the PMMA is not appreciably cross-linked by UVO exposure, there is no strengthening of the surface and hence no statistical change in the thin film moduli. However, reduction in the molecular mass of PMMA *via* chain scission will ultimately lead to a decrease in the modulus. On the basis of the observations shown here, any decrease in average molecular mass from chain scission during a 30 s UVO exposure is insufficient to adversely impact the elastic modulus in comparison to the neat unexposed PMMA. However, UVO treatment is not able to effectively eliminate the observed decrease in the mechanical properties of ultrathin PMMA films. Thus, the data for both PMMA and the low molecular mass PS illustrate the limitations of UVO for improving the elastic modulus at the nanoscale, although UVO is effective for some specific polymer systems such as high molecular mass PS.

Stiffening of polymers at the nanoscale is important for nanotechnology as polymeric materials are commonly utilized as templates.^{10–13} However, PMMA is more commonly utilized in the fabrication of nanostructures than PS,^{11,29,39} so UVO treatment will not be appli-

cable in most cases. Thus other routes to improve the stiffness of polymers are necessary in these cases. One potential alternative to UVO treatment for mechanically reinforcing polymers at the nanoscale is through the addition of an antiplasticizer. Traditionally, small molecule diluents known as plasticizers are added to polymer materials to increase processability and reduce fragility/brittleness by reducing T_g . However, the addition of plasticizers also lead to a decrease in the modulus, which can be detrimental for some applications. Conversely, antiplasticization can occur at low diluent levels when a strong interaction is present between the small molecule and the polymer that leads to densification.^{62–64} In cases where antiplasticization occurs, the increased physical density of the material leads to an increased elastic modulus, despite a decrease in T_g from the addition of the diluent to the polymer.^{62–64} Simulations by de Pablo and co-workers indicate that antiplasticizers can also provide enhanced mechanical rigidity of polymers at the nanoscale.⁴³ Additionally, the antiplasticizer homogenizes the polymer film in terms of cooperative rearrangement,⁴³ this homogenization eliminates surface effects³⁷ that have been attributed as the cause for a decrease in T_g ³² and mechanical properties³⁴ of nanoconfined polymers. Recently, an antiplasticizer has been shown to improve the mechanical stability of PMMA nanostructures.⁴⁵ A maximum in the apparent modulus occurs at approximately 5% by mass of antiplasticizer, but for a fixed composition, the moduli of the PMMA decreases as the feature size is decreased;⁴⁵ this result is consistent with the aforementioned simulations where antiplasticizing diluents homogenize the film.⁴³ Conversely, Ellison *et al.* showed that the addition of approximately 9% by mass pyrene in PS eliminated any size dependencies on the film T_g behavior.⁴⁷ Potential $\pi-\pi$ interactions between PS and pyrene could lead to an antiplasticization effect. However, addition of only 4% by mass DOP to PS also eliminates nanoconfinement effects on thin film T_g .⁴⁷ This result is quite curious, as addition of DOP to bulk polymers leads to plasticization with a reduction in the bulk T_g and a decrease in the elastic modulus.^{65,66} However, the loss of thickness dependence in T_g for PS thin films is not consistent with the experimental data for the mechanical properties of PMMA nanostructures with added antiplasticizer,⁴⁵ thus it is important to understand how DOP or other plasticizers impact the modulus of polymers at the nanoscale.

For ≈ 55 nm PS thin films, a decrease in both T_g and elastic modulus is observed with the addition of DOP. Without DOP, the T_g of the PS ($M_n = 2.3$ kg/mol) is 64.3 ± 1.6 °C, but T_g decreases to 55.1 ± 2.1 °C with the addition of 5% by mass DOP. This depression in T_g is consistent with previous data for the T_g of DOP-plasticized PS in the bulk.⁶⁷ Figure 3 illustrates the slight decrease in elastic modulus of PS films ($h_f \approx 55$ nm) as the concentration of DOP is increased. The decrease in both T_g and elastic modulus with addition of DOP in the films is indicative of plasticization of the PS at 55 nm.

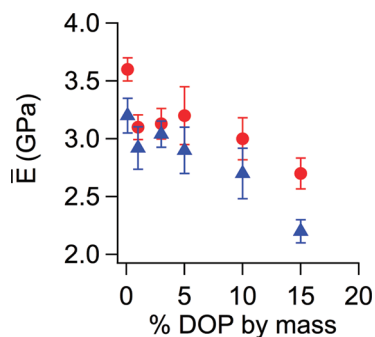


Figure 3. Modulus dependency on DOP concentration for both 990 kg/mol (●) and 2.3 kg/mol (▲) PS films ($h_f = 55$ nm). The error bars represent one standard deviation of the data, which is taken as the experimental uncertainty of the measurement.

However, the addition of DOP to 990 kg/mol PS thin films leads to a progressive increase in the modulus for films less than ≈ 50 nm thick, as shown in Figure 4. It is interesting that the bulk modulus is not significantly impacted by the addition of up to 5% by mass DOP, but the modulus of ultrathin (< 30 nm) films is strongly dependent upon the DOP concentration over the same range. At 5% by mass DOP, the PS film modulus is statistically independent of film thickness. Increasing the DOP concentration to 10 and 15% by mass leads to a slight decrease in the modulus, but the elastic modulus remains independent of film thickness at higher concentrations. This is reminiscent of the impact of DOP on the T_g of PS thin films where bulk T_g is recovered in ultrathin films if greater than 4% by mass DOP is added,⁴⁷ although the length scale at which T_g and modulus deviations from bulk occur is not always consistent.^{21,31} The addition of nonvolatile diluents appears to be a facile mechanism to improve the elastic modulus of polymers at the nanoscale. However, the effect of UVO treatment on the mechanical behavior of both high and low molecular mass PS thin films is strikingly different, so it would be insightful to determine if similar differences exist when adding DOP to these systems. One issue that arises is the initial low T_g of the 1.3 kg/mol PS; addition of 5% by mass DOP decreases T_g below ambient, thus precluding the formation of stable wrinkle patterns to elucidate the thin film modu-

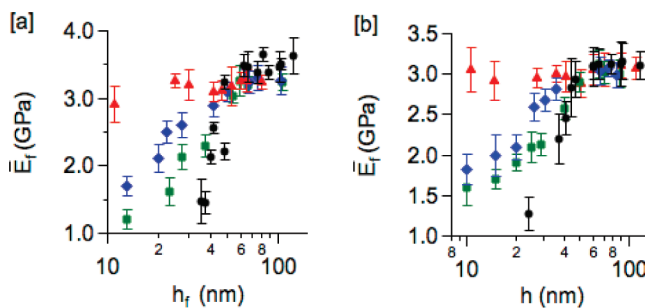


Figure 4. Modulus of (a) 990 kg/mol and (b) 2.3 kg/mol PS with varying DOP concentration: pure PS (●), 1% by mass (■), 3% by mass (◆), and 5% by mass (▲). The error bars represent one standard deviation of the data, which is taken as the experimental uncertainty of the measurement.

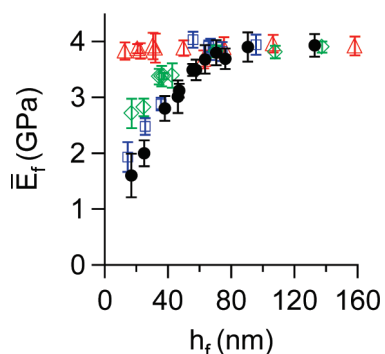


Figure 5. Modulus of 91 kg/mol PMMA with varying DOP concentration: pure polymer (●), 1% by mass (□), 3% by mass (◇), and 5% by mass (△). The error bars represent one standard deviation of the data, which is taken as the experimental uncertainty of the measurement.

lus. Instead, a slightly larger molar mass is utilized for the DOP studies (2.3 kg/mol). As shown in Figure 4b, the addition of DOP to this lower molecular mass PS also yields improvements in the modulus of the ultrathin films. The impact of DOP on the modulus is identical between the two molecular masses. This suggests that the mode of inhibition of nanoconfinement effects by addition of DOP is independent of the degree of mechanical heterogeneity within the film as the thickness of soft surface layer (δ) is estimated to be nearly double for the 2.3 kg/mol PS in comparison to the 990 kg/mol PS.³¹

To further examine the inhibition of nanoconfinement effects on polymer moduli by addition of DOP, a polymer lacking aromaticity is examined: PMMA. Figure 5 shows the film thickness dependence of the modulus of PMMA as a function of DOP concentration. Similar to the observed behavior for PS, addition of DOP systematically increases the modulus of ultrathin films of PMMA. At 5% by mass DOP, the modulus of the PMMA is independent of film thickness, just as seen for PS films. These results suggest that small molecules in ultrathin polymer films may be able to act as antiplasticizers, even if these diluents are plasticizers in the bulk. One alternative explanation to the increased modulus for the ultrathin films with added plasticizer is a similar effect to the initial increase in elastic modulus from swelling of a cross-linked polymer network.⁶⁸ In the network, the rubbery chains are confined by the chemical cross-links during swelling, which is a competition between entropy of mixing and chain stretching. For the thin films, there is ample evidence in the literature for a

rubber-like surface.^{23,32,35–37} physical cross-links near the surface that form loops that are locked within the film (glass) could behave similar to the chemical cross-links of swollen networks. However, the low M_n PS examined here is below the entanglement M_n but still exhibits a thickness-independent moduli with 5% by mass DOP. These results using a bulk plasticizer to antiplasticize ultrathin films are striking, but it is unclear exactly how the addition of a diluent to a polymer thin film can increase its modulus. This behavior could be rationalized by molecular dynamics simulations that suggest thin films containing a small molecule exhibit smaller-scale collective motion, which reduces the influence of the free surface layer and subsequently leads to eliminating the bulk modulus reduction that is present in the neat polymer film.⁴⁴ Additional theoretical work is necessary to understand how the addition of DOP to PS and PMMA thin films eliminates thickness dependence of elastic modulus.

CONCLUSIONS

The elastic moduli of PS and PMMA are found to decrease when the film thickness is less than 50 nm as a result of a mechanically compliant surface layer. Two strategies to limit or circumvent the reduction in modulus of polymers at the nanoscale are examined: UV–ozone-promoted oxidation/cross-linking of surface and addition of small molecule diluent. UVO exposure leads to oxidation and cross-linking of the near surface of PS (≈ 5 nm), which leads to an overall increase in modulus. For high molecular mass PS (492 kg/mol), the thickness of the cross-linked layer is similar to that of a soft free surface layer ($\delta \approx 5$ nm) and the modulus of these films after UVO exposure is independent of film thickness. For low molecular mass PS (1.3 kg/mol), the free surface layer ($\delta \approx 25$ nm) is larger than the depth of surface modification, thus the modulus for this low molecular mass PS is still thickness-dependent after UVO exposure. Due to chain scission during the photodegradation process for PMMA, no statistical variation in the modulus compared to the pure nanoconfined polymer is observed with UVO exposure. Conversely, addition of a plasticizer for bulk PS and PMMA leads to a reduction in the extent of decrease in moduli for ultrathin films. At 5% by mass DOP, the moduli of PS and PMMA films are independent of film thickness. This result suggests that the polymers are antiplasticized by DOP at the nanoscale despite DOP acting as a plasticizer in the bulk for both PMMA and PS.

METHODS

Certain commercial materials and equipment are identified in this paper in order to specify adequately the experimental procedure. In no case does such identification imply recommendation by the National Institute of Standards and Technology nor does it imply that the material or equipment identified is necessarily the best available for this purpose.

PS of varying molecular mass was purchased from Polymer Laboratories ($M_n = 1.3$ kg/mol, $T_g = 29.9$ °C; $M_n = 2.3$ kg/mol,

$T_g = 64.3$ °C; $M_n = 492$ kg/mol, $T_g = 106.1$ °C; $M_n = 990$ kg/mol, $T_g = 106.3$ °C). PMMA was purchased from Polymer Source ($M_w = 91$ kg/mol, $T_g = 105$ °C). Dioctyl phthalate (DOP) and toluene were purchased from Aldrich and used as received.

Silicon wafers (450 μm thick) were used as substrates for PS, cleaved into approximately 2.5 cm \times 1 cm pieces and cleaned with UVO (model 42, Jelight). To assist with film transfer, mica sheets were used as substrates for PMMA films. Polymer films were spin-cast from the dilute solutions in toluene

onto these substrates. PDMS (Sylgard 184, Dow Corning) was prepared in a ratio of 20:1 by mass of base to curing agent, cast into 1.5 mm thick sheets, and allowed to gel at room temperature for 3 h before curing at 100 °C for 2 h. After cooling to ambient, the PDMS was cut into approximately 2.5 cm × 7.5 cm strips. The modulus of the PDMS was determined using a Texture Analyzer (TA-TX Plus) at a strain rate of 0.01 mm/s and found to be 0.6 ± 0.2 MPa.

In order to exceed the critical strain required to produce surface wrinkling on all samples, the PDMS was prestrained to 4% using a stage described previously.⁶⁹ The polymer film was then transferred to strained PDMS using differential adhesion in water. The sample was dried under vacuum at 10 °C below its bulk T_g to avoid thermal-induced wrinkling. In cases where UVO treatment was used, the polymer film on the strained PDMS was exposed to UVO (model 42, Jelight) at a distance of approximately 10 mm from the UV source for a controlled period of time. This UVO outputs light from a low-pressure mercury vapor lamp with a nominal intensity of 28 mW/cm² at 254 nm, so exposure dosage between 0.84 and 2.52 J/cm² was used in this study (corresponding to 30–90 s of exposure). The prestrain on the PDMS was then released at a rate of 0.1 mm/s. All samples were released at ambient temperature ($T = 22 \pm 2$ °C). Euler-type wrinkling occurs upon compression of the polymer film by release of the prestrain. Due to a minimization of the total strain energy, the resulting surface is composed of sinusoidal undulations having a dominant wavelength, λ . As the PDMS substrate is much thicker than the film and the modulus of the film is much greater than the modulus of the substrate, the mechanics can be solved using a semi-infinite plane approximation that results in the wavelength being independent of strain as long as the substrate is linear elastic.⁶⁹ This strain invariance of λ results in a simple route to deduce the thin film modulus, \bar{E}_f , if the modulus of the substrate, \bar{E}_s , and the film thickness, h_f , are known. The relationship between the film modulus and the wrinkling wavelength is given by $\bar{E}_f = 3\bar{E}_s(\lambda/2\pi h_f)^3$.

The thickness of the polymer film on the strained PDMS was determined using a variable angle spectroscopic ellipsometer (VASE M-2000, J.A. Woollam Co., Inc.) over a wavelength range from 250 to 1700 nm using three incident angles, 67, 70, and 73°. The data were modeled using the optical properties of the PDMS substrate and a Cauchy layer to describe the polymer film. The film thickness measured before transfer (*i.e.*, on the silicon wafer) was found to be within 1 nm of the film thickness after transfer (*i.e.*, on PDMS). Additionally, the decrease in film thickness from UVO exposure is less than 1.5 nm in all cases examined.

Characterization of the wrinkled surfaces was performed using atomic force microscopy (AFM) and optical microscopy. AFM images were acquired at ambient temperature on an Agilent Technologies 5500 system in tapping mode using a constant scan size of 7.5 μm × 7.5 μm at a scan rate of 1 Hz. AFM images were analyzed using 1D fast Fourier transform (FFT) to obtain the wavelength of the wrinkles. Optical images were acquired using a Mitutoyo Ultraplano FS-110 and analyzed using 1D FFT to determine the wrinkle wavelength.

To measure the T_g of PS with 5% by mass of DOP as thin films on PDMS, 20:1 PDMS films were spin-cast onto clean silicon wafers from a dilute toluene solution (0.5–2% by mass PDMS) and cured at 100 °C for 2 h. The PDMS layer was varied from 30 to 70 nm thick. PS films containing 5% by mass of DOP ($h_f \approx 55$ nm) were transferred to the PDMS films from silicon wafers as described above. Ellipsometry was used to measure the thermal response of PDMS films and PDMS/PS-DOP bilayers. T_g was determined from changes in the PS-DOP film thickness measured upon cooling from 60 to 30 °C at 1.0 °C/min in a nitrogen purge atmosphere.

Acknowledgment. We gratefully acknowledge the use of facilities within the LeRoy Eyring Center for Solid State Science at Arizona State University. The authors thank B. O'Brien for assistance with AFM measurements. This manuscript is an official contribution of the National Institute of Standards and Technology.

Supporting Information Available: Data illustrating the stability of the DOP within the films as determined by thin film T_g and the elastic modulus of PS films containing >10 wt % DOP are included. This material is available free of charge via the Internet at <http://pubs.acs.org>.

REFERENCES AND NOTES

- Autumn, K.; Liang, Y. A.; Hsieh, S. T.; Zesch, W.; Chan, W. P.; Kenny, T. W.; Fearing, R.; Full, R. J. Adhesive Force of a Single Gecko Foot-Hair. *Nature* **2000**, *405*, 681–685.
- Geim, A. K.; Dubonos, S. V.; Grigorieva, I. V.; Novoselov, K. S.; Zhukov, A. A.; Shapoval, S. Y. Microfabricated Adhesive Mimicking Gecko Foot-Hair. *Nat. Mater.* **2003**, *2*, 461–463.
- Blossey, R. Self-Cleaning Surfaces—Virtual Realities. *Nat. Mater.* **2003**, *2*, 301–306.
- Cheng, Y. T.; Rodak, D. E.; Wong, C. A.; Hayden, C. A. Effects of Micro- and Nano-structures on the Self-Cleaning Behavior of Lotus Leaves. *Nanotechnology* **2006**, *17*, 1359–1362.
- Feng, L.; Li, S.; Li, Y.; Li, H.; Zhang, L.; Zhai, J.; Song, Z. Y.; Jiang, L. L.; Zhu, D. Super-Hydrophobic Surfaces: From Natural to Artificial. *Adv. Mater.* **2002**, *14*, 1857–1860.
- Carman, M. L.; Estes, T. G.; Feinber, A. W.; Schumacher, J. F.; Wilkerson, W.; Wilson, L. H.; Callow, M. E.; Callow, J. A.; Brennan, A. B. Engineered Antifouling Microtopographies—Correlating Wettability with Cell Attachment. *Biofouling* **2006**, *22*, 11–21.
- Ahmand, C. S.; Gerdner, T. R.; Groh, M.; Arnouk, J.; Levine, W. N. Mechanical Properties of Soft Tissue Femoral Fixation Devices for Anterior Cruciate Ligament Reconstruction. *Am. J. Sports Med.* **2004**, *32*, 635–640.
- Espinosa, H. D.; Prorok, B. C.; Fischer, M. A. Methodology for Determining Mechanical Properties of Freestanding Thin Films and MEMS Materials. *J. Mech. Phys. Solids* **2002**, *51*, 47–67.
- Kim, J. S.; Granstrom, M. Indium-Tin Oxide Treatments for Single- and Double-Layer Polymeric Light-Emitting Diodes: The Relation between the Anode Physical, Chemical, and Morphological Properties and the Device Performance. *J. Appl. Phys.* **1998**, *84*, 6859–6870.
- Ozin, G. A.; Yang, S. M. The Race for the Photonic Chip: Colloidal Crystal Assembly in Silicon Wafers. *Adv. Funct. Mater.* **2001**, *11*, 95–104.
- Hartschuh, R.; Ding, Y.; Roh, J. H.; Kisliuk, A.; Sokolov, A. P.; Soles, C. L.; Jones, R. L.; Hu, T. J.; Wu, W. L.; Mahorowala, A. P. Brillouin Scattering Studies of Polymeric Nanostructures. *J. Polym. Sci., Part B* **2004**, *42*, 1106–1113.
- Wung, C. J.; Pang, Y.; Prasad, P. N.; Karasz, F. E. Poly(*p*-phenylene vinylene)—Silica Composite: A Novel Sol—Gel Processed Non-linear Optical Material for Optical Waveguides. *Polymer* **1991**, *32*, 605–608.
- Lei, J.; Fan, J.; Yu, C. Z.; Zhang, L. Y.; Jiang, S. Y.; Tu, B.; Zhao, D. Y. Immobilization of Enzymes in Mesoporous Materials: Controlling the Entrance to Nanoscale. *Microporous Mesoporous Mater.* **2004**, *73*, 121–128.
- Ellison, C. J.; Torkelson, J. M. The Distribution of Glass-Transition Temperatures in Nanoscopically Confined Glass Formers. *Nat. Mater.* **2003**, *2*, 695–700.
- Forrest, J. A.; Mattsson, J. Reductions of the Glass Transition Temperature in Thin Polymer Films: Probing the Length Scale of Cooperative Dynamics. *Phys. Rev. E* **2000**, *61*, R53–R56.
- Keddie, J. L.; Jones, R. A. L. Size-Dependent Depression of the Glass Transition Temperature in Polymer Films. *Europhys. Lett.* **1994**, *27*, 59–64.
- Kim, J. H.; Jang, J.; Zin, W. C. Estimation of the Thickness Dependence of the Glass Transition Temperature in Various Thin Polymer Films. *Langmuir* **2000**, *16*, 4064–4067.
- Torres, J. A.; Nealey, P. F.; de Pablo, J. J. Molecular Simulation of Ultrathin Polymeric Films near the Glass Transition. *Phys. Rev. Lett.* **2000**, *85*, 3221–3224.
- Tweedie, C. A.; Constantinides, G.; Lehman, K. E.; Brill, D. J.

- Blackman, G. S.; Van Vliet, K. J. Enhanced Stiffness of Amorphous Polymer Surfaces under Confinement of Localized Contact Loads. *Adv. Mater.* **2007**, *19*, 2540–2546.
20. Stafford, C. M.; Vogt, B. D.; Harrison, C.; Julthongpipit, D.; Huang, R. Elastic Moduli of Ultrathin Amorphous Polymer Films. *Macromolecules* **2006**, *39*, 5095–5099.
 21. Torres, J. M.; Stafford, C. M.; Vogt, B. D. Elastic Modulus of Amorphous Polymer Thin Films: Relationship to the Glass Transition Temperature. *ACS Nano* **2009**, *3*, 2677–2685.
 22. Miyake, K.; Satomi, N.; Sasaki, S. Elastic Modulus of Polystyrene Film from Near Surface to Bulk Measured by Nanoindentation Using Atomic Force Microscopy. *Appl. Phys. Lett.* **2006**, *89*, 031925.
 23. Meyers, G. F.; Dekoven, B. M.; Seitz, J. T. Is the Molecular Surface of Polystyrene Really Glassy? *Langmuir* **1992**, *8*, 2330–2335.
 24. Forrest, J. A.; Dalnoki-Veress, K.; Dutcher, J. R. Brillouin Light Scattering Studies of the Mechanical Properties of Thin Freely Standing Polystyrene Films. *Phys. Rev. E* **1998**, *58*, 6109–6114.
 25. O'Connell, P. A.; McKenna, G. B. Rheological Measurements of the Thermoviscoelastic Response of Ultrathin Polymer Films. *Science* **2005**, *307*, 1760–1763.
 26. O'Connell, P. A.; Hutcheson, S. A.; McKenna, G. B. Creep Behavior of Ultrathin Polymer Films. *J. Polym. Sci., Part B* **2008**, *46*, 1952–1965.
 27. Alcoutlabi, M.; McKenna, G. B. Effects of Confinement on Material Behavior at the Nanometer Size Scale. *J. Phys.: Condens. Matter* **2005**, *17*, R461–R524.
 28. Tsui, O. K. C.; Russell, T. P.; Hawker, C. J. Effect of Interfacial Interactions on the Glass Transition of Polymer Thin Films. *Macromolecules* **2001**, *34*, 5535–5539.
 29. Stoykovich, M. P.; Yoshimoto, K.; Nealey, P. F. Mechanical Properties of Polymer Nanostructures: Measurements Based on Deformation in Response to Capillary Forces. *Appl. Phys. A: Mater. Sci. Process.* **2008**, *90*, 277–283.
 30. Bohme, T. R.; de Pablo, J. J. Evidence for Size-Dependent Mechanical Properties from Simulations of Nanoscopic Polymeric Structures. *J. Chem. Phys.* **2002**, *116*, 9939–9951.
 31. Torres, J. M.; Stafford, C. M.; Vogt, B. D. Impact of Molecular Mass on the Elastic Modulus of Thin Polystyrene Films. *Polymer* **2010**, doi: 10.1016/j.polymer.2010.07.003.
 32. Forrest, J. A.; Dalnoki Veress, K.; Stevens, J. R.; Dutcher, J. R. Effect of Free Surfaces on the Glass Transition Temperature of Thin Polymer Films. *Phys. Rev. Lett.* **1996**, *77*, 2002–2005.
 33. Pu, Y.; Rafailovich, M. H.; Sokolov, J.; Gersappe, D.; Peterson, T.; Wu, W. L.; Schwarz, S. A. Mobility of Polymer Chains Confined at a Free Surface. *Phys. Rev. Lett.* **2001**, *87*, 206101.
 34. Chakravartula, A.; Komvopoulos, K. Viscoelastic Properties of Polymer Surfaces Investigated by Nanoscale Dynamic Mechanical Analysis. *Appl. Phys. Lett.* **2006**, *88*, 131901.
 35. Knoll, A.; Wiesmann, D.; Gotsmann, B.; Duerig, U. Relaxation Kinetics of Nanoscale Indents in a Polymer Glass. *Phys. Rev. Lett.* **2009**, *102*, 117801.
 36. Qi, D.; Fakhraai, Z.; Forrest, J. A. Substrate and Chain Size Dependence of Near Surface Dynamics of Glassy Polymers. *Phys. Rev. Lett.* **2008**, *101*, 096101.
 37. Fakhraai, Z.; Forrest, J. A. Measuring the Surface Dynamics of Glassy Polymers. *Science* **2008**, *319*, 600–604.
 38. Wallace, W. E.; Fischer, D. A.; Efimenko, K.; Wu, W. L.; Genzer, J. Polymer Chain Relaxation: Surface Outpaces Bulk. *Macromolecules* **2001**, *34*, 5081–5082.
 39. Mundra, M. K.; Donthu, S. K.; Dravid, V. P.; Torkelson, J. M. Effect of Spatial Confinement on the Glass-Transition Temperature of Patterned Polymer Nanostructures. *Nano Lett.* **2007**, *7*, 713–718.
 40. Lee, K.; Pan, F.; Carroll, G. T.; Turro, N. J.; Koberstein, J. T. Photolithographic Technique for Direct Photochemical Modification and Chemical Micropatterning of Surfaces. *Langmuir* **2004**, *20*, 1812–1818.
 41. Klein, R. J.; Fischer, D. A.; Lenhart, J. L. Systematic Oxidation of Polystyrene by Ultraviolet–Ozone, Characterized by Near-Edge X-ray Absorption Fine Structure and Contact Angle. *Langmuir* **2008**, *24*, 8187–8197.
 42. Teare, D. O. H.; That-Ton, C.; Bradley, R. H. Surface Characterization and Ageing of Ultraviolet–Ozone-Treated Polymers Using Atomic Force Microscopy and X-ray Photoelectron Spectroscopy. *Surf. Interface Anal.* **2000**, *29*, 276–283.
 43. Riggelman, R. A.; Yoshimoto, K.; Douglas, J. F.; de Pablo, J. J. Influence of Confinement on the Fragility of Antiplasticized and Pure Polymer Films. *Phys. Rev. Lett.* **2006**, *97*, 045502.
 44. Riggelman, R. A.; Douglas, J. F.; de Pablo, J. J. Tuning Polymer Melt Fragility with Antiplasticizer Additives. *J. Chem. Phys.* **2007**, *126*, 234903.
 45. Delcambre, S. P.; Riggelman, R. A.; de Pablo, J. J.; Nealey, P. F. Mechanical Properties of Antiplasticized Polymer Nanostructures. *Soft Matter* **2010**, *6*, 2475–2483.
 46. Tan, L.; Kong, Y. P.; Pang, S. W.; Yee, A. F. Imprinting of Polymer at Low Temperature and Pressure. *J. Vac. Sci. Technol., B* **2004**, *22*, 2486–2492.
 47. Ellison, C. J.; Ruzskowski, R. L.; Fredin, N. J.; Torkelson, J. M. Dramatic Reduction of the Effect of Nanoconfinement on the Glass Transition of Polymer Films via Addition of Small-Molecule Diluent. *Phys. Rev. Lett.* **2004**, *92*, 095702.
 48. Stafford, C. M.; Harrison, C.; Beers, K. L.; Karim, A.; Amis, E. J.; Vanlandingham, M. R.; Kim, H. C.; Volksen, W.; Miller, R. D.; Simonyi, E. A. A Buckling-Based Metrology for Measuring the Elastic Moduli of Polymeric Thin Films. *Nat. Mater.* **2004**, *3*, 545–550.
 49. Huang, R.; Stafford, C. M.; Vogt, B. D. Effect of Surface Properties on Wrinkling of Ultrathin Films. *J. Aerospace Eng.* **2007**, *20*, 38–44.
 50. Priestley, R. D.; Ellison, C. J.; Broadbelt, L. J.; Torkelson, J. M. Structural Relaxation of Polymer Glasses at Surfaces, Interfaces, and In Between. *Science* **2005**, *309*, 456–459.
 51. Efremov, M. Y.; Olson, E. A.; Zhang, M.; Zhang, Z.; Allen, L. H. Glass Transition in Ultrathin Polymer Films: Calorimetric Study. *Phys. Rev. Lett.* **2003**, *91*, 085703.
 52. Ellison, C. J.; Mundra, M. K.; Torkelson, J. M. Impacts of Polystyrene Molecular Weight and Modification to the Repeat Unit Structure on the Glass Transition–Nanoconfinement Effect and the Cooperativity Length Scale. *Macromolecules* **2005**, *38*, 1767–1778.
 53. Callen, B. W.; Ridge, M. L.; Lahooti, S.; Neumann, A. W.; Sodhi, R. N. S. Remote Plasma and Ultraviolet–Ozone Modification of Polystyrene. *J. Vac. Sci. Technol., A* **1995**, *13*, 2023–2029.
 54. Nie, N. Y.; Wlazak, M. J.; Berno, B.; McIntyre, N. S. Atomic Force Microscopy of Polypropylene Surfaces Treated by UV and Ozone Exposure: Modification of Morphology and Adhesion Force. *Appl. Surf. Sci.* **1999**, *144–145*, 627–632.
 55. Zhang, R.; Cherdhirankorn, T.; Graf, K.; Koynov, K.; Berger, R. Swelling of Cross-Linked Polystyrene Beads in Toluene. *Microelectron. Eng.* **2008**, *85*, 1261–1264.
 56. Zhang, D.; Dougal, S. M.; Yeganeh, M. S. Effects of UV Irradiation and Plasma Treatment on a Polystyrene Surface Studied by IR–Visible Sum Frequency Generation Spectroscopy. *Langmuir* **2000**, *16*, 4528–4532.
 57. Otocka, E. P.; Curran, S.; Porter, R. S. Photo-oxidation of Polystyrene—Irradiation at 254 and 365 nm. *J. Appl. Polym. Sci.* **1983**, *28*, 3227–3233.
 58. Efimenko, K.; Wallace, W. E.; Genzer, J. Surface Modification of Sylgard-184 Poly(dimethyl siloxane) Networks by Ultraviolet and Ultraviolet/Ozone Treatment. *J. Colloid Interface Sci.* **2002**, *254*, 306–315.
 59. Thurn-Albrecht, T.; Schotter, J.; Kastle, C. A.; Emley, N.; Shibauchi, T.; Krusin-Elbaum, L.; Guarini, K.; Black, C. T.; Tuominen, M. T.; Russell, T. P. Ultrahigh-Density Nanowire Arrays Grown in Self-Assembled Diblock Copolymer Templates. *Science* **2000**, *290*, 2126–2129.
 60. Choi, J. O.; Moore, J. A.; Correlli, J. C.; Silverman, J. P. Degradation of Poly(methylmethacrylate) by Deep Ultraviolet, X-ray, Electron Beam, and Proton Beam Irradiations. *J. Vac. Sci. Technol., B* **1988**, *6*, 2286–2289.

61. Lee, E. H.; Mansur, L. K. LET Effect on Cross-Linking and Scission Mechanisms of PMMA During Irradiation. *Radiat. Phys. Chem.* **1999**, *55*, 293–305.
62. Jackson, W. J.; Caldwell, J. R. Antiplasticization 0.2. Characteristics of Antiplasticizers. *J. Appl. Polym. Sci.* **1967**, *11*, 211–226.
63. Jackson, W. J.; Caldwell, J. R. Antiplasticization 0.3. Characteristics and Properties of Antiplasticizable Polymers. *J. Appl. Polym. Sci.* **1967**, *11*, 227–244.
64. Zerda, A. S.; Lesser, A. J. Organophosphorous Additive for Fortification, Processibility, and Flame Retardance of Epoxy Resins. *J. Appl. Polym. Sci.* **2002**, *84*, 302–309.
65. Cowie, J. M. G. *Polymers: Chemistry and Physics of Modern Materials*; Thorne: Cheltenham, UK, 1998.
66. Ferry, J. D. *Viscoelastic Properties of Polymers*; John Wiley and Sons: New York, 1980.
67. Chiou, J. S.; Barlow, J. W.; Paul, D. R. Plasticization of Glassy Polymers by CO₂. *J. Appl. Polym. Sci.* **1985**, *30*, 2633–2642.
68. Gottlieb, M.; Gaylord, R. J. Experimental Tests of Entanglement Models of Rubber Elasticity 2. Swelling. *Macromolecules* **1984**, *17*, 2024–2030.
69. Stafford, C. M.; Guo, S.; Harrison, C.; Chiang, M. Y. M. Combinatorial and High-Throughput Measurements of the Modulus of Thin Polymer Films. *Rev. Sci. Instrum.* **2005**, *76*, 062207.